Proceedings of the 37th National & 4th International Conference on Fluid Mechanics and Fluid Power
December 16-18, 2010, IIT Madras, Chennai, India.

FMFP10 - CF - 17

A STUDY ON THE INFLUENCE OF GAP RATIO ON TURBULENT FLOW PAST TWO EQUAL SIZED SQUARE CYLINDERS PLACED SIDE-BY-SIDE

M.B.Shyam Kumar
Ph.D Research Scholar
Fluid Mechanics Laboratory
Department of Applied Mechanics
Indian Institute of Technology, Madras
Chennai-600 036, Tamilnadu, India
mbshyamme@gmail.com

S.Vengadesan
Associate Professor
Fluid Mechanics Laboratory
Department of Applied Mechanics
Indian Institute of Technology, Madras
Chennai-600 036, Tamilnadu, India
vengades@iitm.ac.in

ABSTRACT

A uniform flow past two infinitely long equal sized square cylinders arranged in a side-by-side pattern has been investigated using Large Eddy Simulation (LES) technique. The Reynolds number (Re) based on the square cylinder diameter (D) and the free-stream velocity (U_∞) is 50,000. The modelling of sub-grid scales of turbulence is done using the standard Smagorinsky model. The effect of transverse gap ratio (T/D) on the flow characteristics has been studied in detail. An in-house code employing finite difference scheme with staggered grid arrangement is used to discretize the governing equations. The numerical simulations are carried out for five different T/D ratios, namely 1.120, 1.250, 1.375, 1.750 and 3.000. The results in terms of the mean and RMS values of the lift and drag coefficients, Strouhal number, mean base pressure coefficient and contours of streamlines, vorticity and cylinder surface pressure distributions are presented.

Keywords: Square cylinder, Side-by-side, Turbulence, Vortex shedding, Large Eddy Simulation

INTRODUCTION

Flow interference brought about by the two bluff bodies placed in side-by-side arrangement results in a very complex flow pattern. The complexity lies in the interaction of four separated free shear layers, two Karman vortex formation and shedding processes and interactions between two Karman vortex streets. These cylinder-like structures in air and water flows, find many applications which include high rise building, technical structures such as chimneys, cooling towers, electrical pylons, struts, bridges and marine risers. The aerodynamic forces acting on the two structures are quite different from those acting on a single structure. Wong et al., 1995 presented experimental results for flow past two side-by-side square cylinders of unequal size at Re=50000. The gap side shear layer of the large cylinder reattaches to its inner surface for smaller separation. For larger separation, reattachment of the gap side shear layer was found in the inner surface of the small cylinder. Skewed flow towards the small cylinder was seen at smaller gap ratios and no bistable flow was observed. As the separation increases the skewness of the vortex streets decreased.

Kolar et al., 1997 studied the unsteady flow around two identical square cylinders placed side-by-side using laser-Doppler velocimetry and ensemble averaging at Re=23100. Coupled vortex streets with in-antiphase mode exist, along with the flow being symmetric about the centerline. In addition, they found a jet like flow in the gap using the time averaged velocity field. Sumner et al., 1999 reported the fluid dynamics of flow past two and three circular cylinders of equal size arranged side-by-side and found that they are quite insensitive for $500<Re<111000$. At smaller gap ratios in case of two cylinders, the higher momentum fluid through the gap increases the base pressure, reduces the drag and also increases the streamwise extent of the vortex formation region. Sumner et al., 2000

investigated the flow around two equal sized circular cylinders arranged in a staggered pattern using flow visualization and particle image velocimetry. They identified nine different flow patterns and presented the phenomenon of shear layer reattachment, induced separation, vortex pairing and synchronization and vortex impingement. Their study revealed that the vortex shedding frequencies are more properly associated with individual shear layers than with the individual cylinders.

Kondo, 2004 has showed that when the distance between the two rectangular cylinders located in a uniform flow was short, a very complicated flow pattern arises. Kondo and Matsukuma, 2005 reported the phenomena of biased gap flow that appeared when the two circular cylinders placed side-by-side, are at a small separation distance. In addition, they found the flow pattern changing from the biased gap flow to a coupled flow, when the two cylinders are at a larger spacing. Agrawal et al., 2006 investigated the flow around two identical square cylinders placed side-by-side at Re=73 using lattice Boltzmann method. They proved the existence of both synchronized and flip-flop regimes. The merging of wakes was gradual in the synchronized regime and rapid in case of the flip-flop regime. They also observed the occurrence of either in-phase or in-antiphase mode of vortex shedding in both the regimes. Liu and Cui, 2006 reported the three-dimensional flow at Re=200 over two side-by-side circular cylinders. The wake patterns depend not only on Re and gap spacing, but also on the end-flow conditions. They found biasing of the gap flow intermittently towards one cylinder or the other. Niu and Zhu, 2006 presented results for flow past two identical square cylinders in staggered arrangement at Re=250. They examined the influence of the cylinder spacing on the flow induced forces and vortex shedding frequencies and the effect of primary wake interference on the secondary flow structure. They reported that the momentum of the gap flow which was transferred into the near wake of one cylinder not only suppresses the oscillations of the drag and lift of that cylinder, but also suppresses the generation of the secondary organized structures in the near wake of that cylinder. In this paper our focus is to investigate numerically the effect of transverse spacing (T/D) on the flow characteristics past two Equal Sized Square Cylinders (ESSC) arranged in a side-by-side pattern. The transverse gap ratio (T/D) is defined as the ratio between the center-to-center distance (T) in the cross-streamwise direction to the cylinder diameter (D). Numerical simulations are carried out for five different T/D ratios namely 1.120, 1.250, 1.375, 1.750 and 3.000. As the flow is unsteady and three-dimensional at high Re number, Large Eddy Simulation (LES) technique is employed for carrying out the study.

MATHEMATICAL FORMULATION

In LES the contribution of large, energy-carrying eddies to momentum or energy transfer is computed exactly, and only the effect of the smallest scales is modelled. To separate the contribution of large scales from the small scales, LES makes use of the filtering operation. Here the grid itself acts as a low pass filter, which is the popularly known implicit filtering approach. Application of a filtering operation to the continuity and Navier-Stokes equations results in the respective filtered governing equations. These equations in non-dimensional tensor form are given by Eq. (1) and (2) respectively as,

$$\frac{\partial \langle u_i \rangle}{\partial x_i} = 0 \qquad (1)$$

$$\frac{\partial \langle u_i \rangle}{\partial t} + \frac{\partial \langle u_i \rangle \langle u_j \rangle}{\partial x_j} = -\frac{\partial \langle p \rangle}{\partial x_i} + \frac{1}{Re}\frac{\partial^2 \langle u_i \rangle}{\partial x_j \partial x_j} + \frac{\partial \tau_{ij}}{\partial x_j} \qquad (2)$$

Here $\langle u \rangle$ and $\langle p \rangle$ represent the filtered velocity and pressure respectively, $\tau_{ij} = -\langle u_i u_j \rangle + \langle u_i \rangle \langle u_j \rangle$ represents the subgrid turbulence stress and $\langle\ \rangle$ indicates spatial filtering. The indices *i* and *j* = 1, 2, 3 represent the three Cartesian coordinates (x, y, z). All geometrical lengths are normalized with D, velocities with U_∞, physical time with D/U_∞ and the pressure with ρU_∞^2. The turbulent fluctuations are accounted in the filtered equations. In order to close the equations, subgrid turbulence stress modeling is required. The role of the subgrid-scale model should be to remove energy from the resolved motion and dissipate it at the appropriate rate by the unresolved motion. In this model, the subgrid

turbulence stress takes the Boussinesq eddy viscosity form which is given by,

$$\tau_{ij} = -\left(\frac{2}{3} k_s \delta_{ij}\right) + 2\upsilon_G S_{ij} \quad (3)$$

Here $S_{ij} = \frac{1}{2}\left(\frac{\partial \langle u_i \rangle}{\partial x_j} + \frac{\partial \langle u_j \rangle}{\partial x_i}\right)$ is the rate of strain tensor of the filtered velocity, υ_G is the subgrid eddy-viscosity coefficient, k_s is the subgrid turbulence kinetic energy and δ_{ij} is the Kroneckar delta. For υ_G and k_s we use the Smagorinsky, 1963 subgrid-scale model given by Eq. (4) and (5).

$$\upsilon_G = 2\ C_s \Delta^2 \sqrt{S_{ij} S_{ij}} \quad (4) \qquad k_s = \upsilon_G^{\,2} / C_k \Delta^2 \quad (5)$$

In order to resolve viscous sub-layer and to apply the no-slip boundary condition on the wall, the first grid point next to the wall in the normal direction should be set close to the wall in terms of non-dimensional wall distance, which should be less than 20. This point becomes physically closer and closer to the wall, as Re increases. But it is found from approximate calculation for the grid used in this study that the first point was far away from this region. So, Van-Driest type near-wall damping for eddy viscosity is not used. Thus Smagorinsky constants C_s and C_k are being set to the constant values of 0.13 and 0.094 respectively. Δ is the filter width which is the characteristic length scale of the largest subgrid-scale eddies and is taken to be the geometrical average of the grid spacing in the three directions. (i.e.) $\Delta = \Delta x_1 \Delta x_2 \Delta x_3^{\,1/3}$

A typical computational domain along with the boundary conditions used for a transverse spacing of 1.250 is shown in Fig. 1. The flow is from left to right and the origin is positioned at the center of the lower square cylinder. The various boundary conditions employed for the simulations are as follows. At the inlet a constant streamwise velocity ($u=U_\infty=1$) is specified with the other two velocities set to zero. On the surface of the two square cylinders the standard boundary condition of no-slip ($u=v=w=0$) has been employed. On the top and bottom boundaries, free-slip or symmetry ($\partial u/\partial y = \partial w/\partial y = v = 0$) boundary condition is used. At the exit, the convective boundary condition $\partial u_i/\partial t + u_c\ \partial u_i/\partial x = 0$ is used. Here u, v and w represent the velocity components in the x, y and z directions respectively and u_c is the convective velocity. The simulations for the T/D ratios of 1.120, 1.250, 1.375, 1.750 and 3.000 have been carried out using structured grids of size 247 x 41 x 311, 247 x 41 x 318, 247 x 41 x 336, 247 x 41 x 353 and 247 x 41 x 385 respectively, each having a blockage ratio of about 12%. A typical grid generated for T/D = 1.120 is shown in Fig. 2a and a closer view of the grid near the two square cylinders is shown in Fig. 2b. In all the cases, the first grid point is at a distance of 0.01D from the surface of the cylinder. The total number of grid points in x and y directions have been maintained constant for all T/D ratios. As the cylinders are moved apart in the z direction, the grid points in this direction only are varied. In the streamwise and cross-streamwise directions they are stretched gradually going away from the cylinders, on the surface of which grids of uniform spacing is generated. The grid points are uniformly distributed in the spanwise direction.

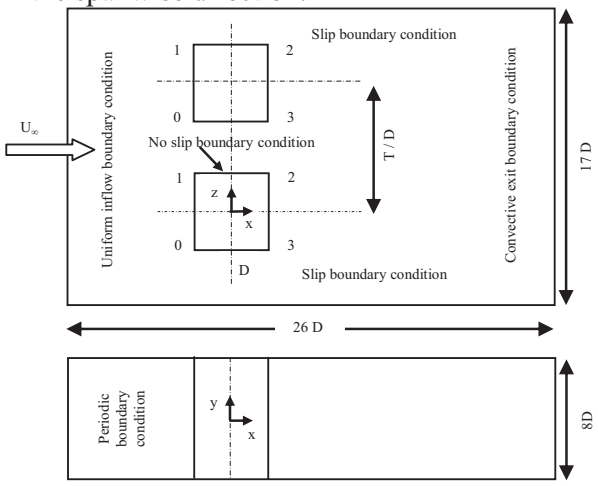

Fig. 1 Computational domain with boundary conditions

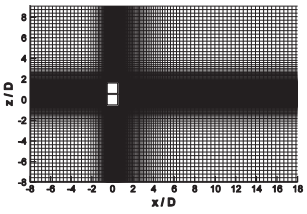

Fig. 2a A grid of size 247x41x311

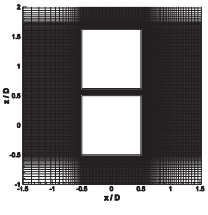

Fig. 2b Zoomed view of the grid

NUMERICAL DETAILS

An in-house code employing finite difference scheme with staggered grid arrangement is used to discretize the governing equations. The velocity components are defined at the midpoint of the cell face to which they are normal and the pressure at the cell center. The viscous and subgrid stress terms are discretized using second order accurate central differencing scheme. The convective terms are discretized by third order upwind biased scheme. The time integration is done by using a second order accurate explicit Adams-Bashforth scheme in two stages. In stage one, the velocity components are found using the previous velocity and pressure values at all cells. These velocities however do not satisfy the divergence free condition for incompressible flow. In order to ensure the mass conservation, adjustments must be made in the stage two. This is achieved by using the Highly Simplified Marker and Cell (HSMAC) algorithm developed by Hirt and Cook, 1972. The non-dimensional time step (dt) to be used, in order to take care of the stability criteria is determined from the Courant-Friedrichs-Lewy condition. A time step of 0.0005 and a convergence limit of 0.0015 were employed for all the simulations. Extensive validation of our computational code has already been carried out for laminar and turbulent flow over an isolated square cylinder. These can be found in Lankadasu and Vengadesan, 2008a, 2008b, 2009, Shyam Kumar and Vengadesan, 2009 for laminar flows and in Nakayama and Vengadesan, 2002, Shyam Kumar and Vengadesan, 2009 for turbulent flows.

RESULTS AND DISCUSSION

The simulations are started with the fluid at rest and then allowed to progress for sufficient time till the flow gets stabilized. The time averaging was performed for the next 20 vortex shedding cycles. Table 1 presents the various bulk parameters namely the mean and RMS values of lift and drag coefficients, Strouhal number (St) and mean base pressure coefficients for flow past two ESSC placed side-by-side at Re=50000. The time history of the lift (Fig. 3a) and drag (Fig. 3b) signals shows high unsteadiness due to the turbulent nature of the flow. It is clear that the lift coefficient acting on the Lower Square Cylinder (LSC) is higher when compared to that of the Upper Square cylinder (USC), for all T/D ratios except for T/D=1.75. Similarly the drag coefficient acting on the USC is higher for all T/D ratios except for the case of T/D=3.0, where it is higher for the LSC. At smaller gap ratios, the amplitude of oscillations seen in the lift and drag signals is small, which is due to the interference of the separated shear layers from the

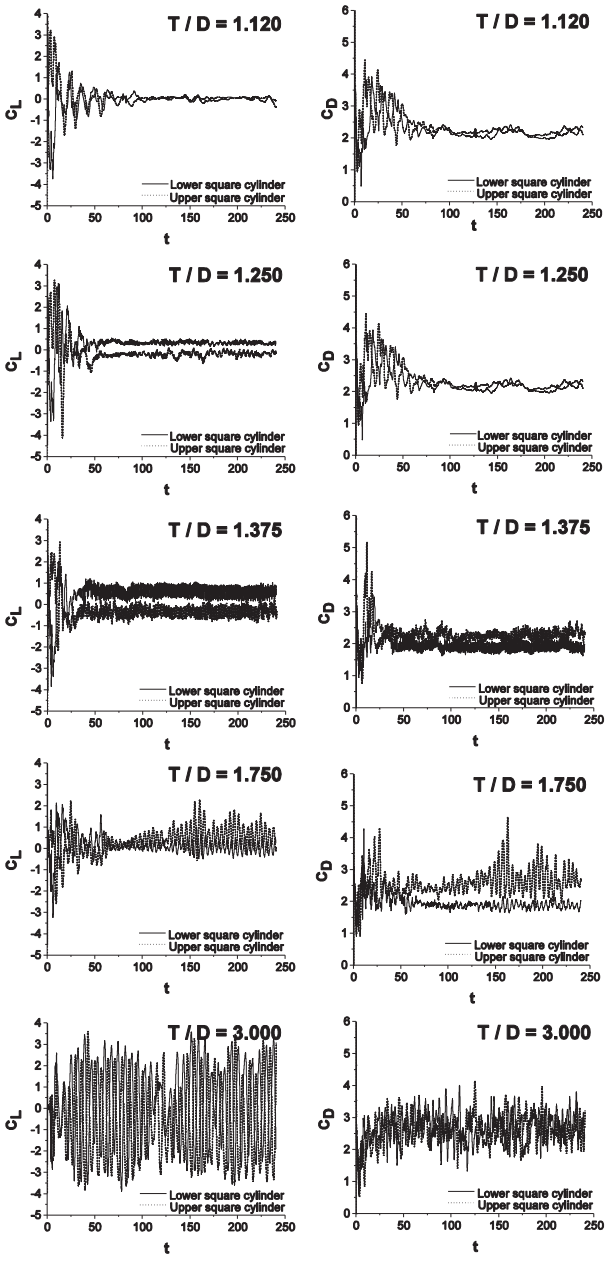

Fig. 3a Time history of the lift signals

Fig. 3b Time history of the drag signals

Table 1 Comparison of bulk parameters at Re=50000

T/D	$\overline{C_{LI}}$	$\overline{C_{LII}}$	C_{LI}^{rms}	C_{LII}^{rms}	$\overline{C_{DI}}$	$\overline{C_{DII}}$	C_{DI}^{rms}	C_{DII}^{rms}	St_I	St_{II}	C_{pbI}	C_{pbII}
1.120	0.072	0.005	0.041	0.093	2.118	2.216	0.105	0.083	0.076	0.015	-1.470	-1.560
1.250	0.342	-0.178	0.068	0.122	1.975	2.201	0.071	0.094	0.015	0.076	-1.322	-1.584
1.375	0.690	-0.404	0.233	0.229	1.874	2.241	0.120	0.124	0.808	0.808	-1.226	-1.592
1.750	0.087	0.633	0.270	0.530	1.881	2.723	0.099	0.426	0.213	0.213	-1.194	-2.114
3.000	0.197	-0.561	1.824	1.881	2.717	2.682	0.420	0.433	0.137	0.152	-2.189	-2.087

Subscript I and II represent the lower and upper cylinder in case of ESSC; Overbar denote mean quantities

gapside of two cylinders. The interference effect starts to vanish as we increase the gap ratio. The vortex shedding process is primarily characterized by $St=(fD)/U_\infty$, where f is the vortex shedding frequency. These are identified based on the dominating frequency in Fig. 4, which is obtained by performing the FFT of the time variation of lift signals. The USC has a larger value of St for T/D=1.25 and 3.0. In case of T/D=1.12, the LSC has a larger value of St. It is identical for both the cylinders in case of T/D=1.375 and 1.75. The multiple peaks seen at smaller gap ratios are due to the existence of other frequencies brought about by the interference effect.

The mean streamline plot for all T/D ratios is shown in Fig. 5. At T/D=1.12, the gapside flow consists of a central jet surrounded by two shear layers separated from the top and bottom corners of the LSC and USC respectively. It is more like a single bluff body flow as reported by Sumner et al., 1999, 2000. Moreover, at this gap ratio the wake is deformed to a maximum extent because of the jet flow from the gapside. The presence of a wide wake behind the LSC and narrow wake behind the USC is clearly seen for T/D=1.25, 1.375 and 1.75. At these gap ratios, the wakes are unsymmetrical in nature. This is because of the biased gapside flow towards the USC. At T/D=3.0, the flow is very similar to that of the isolated square cylinder case. This is justified by the appearance of identical wakes behind the cylinders, which are also symmetrical in nature. Figure 6 shows the mean streamwise velocity plotted at x/D=1.0 location. It attains free stream velocity on the outside of LSC at z/D= -1.5 for all T/D ratios except for T/D=3.0, for which it attains at z/D=-3.0.

In case of the USC, the free stream velocity is attained at z/D=3.0 for all T/D ratios. The jet-like nature of the flow which is more pronounced at smaller gap ratios is also clearly seen. This is justified by the appearance of a closed parabolic velocity profile in the gapside. As the gap ratio increases, we can see the open parabolic velocity profile in the gapside. In other words, one can say that flattening of the parabolic velocity profile in the gapside indicates less interference effect. From this figure, we can also locate the maximum velocity defect point for both the cylinders. As this point moves closer to the cylinder center, the interference effect is absent which is true for T/D=3.0. The distance of the maximum velocity defect point from the corresponding cylinder center decreases as T/D ratio increases. This is similar to what is reported by Wong et al., 1995.

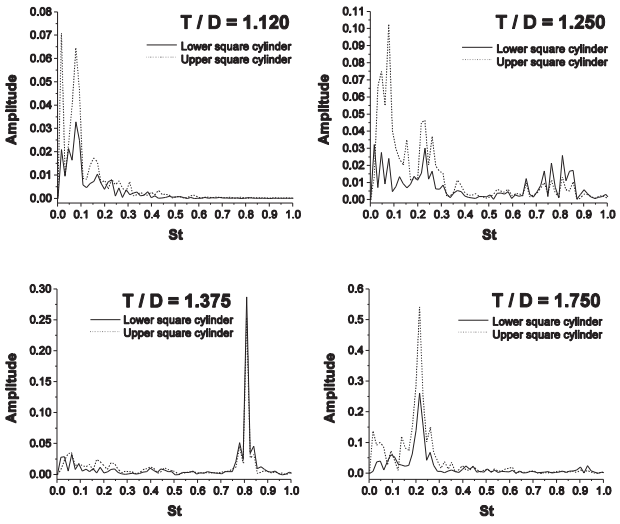

Fig. 4 FFT of the lift signals

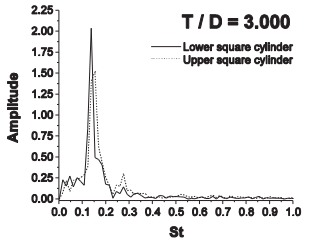

Fig. 4 FFT of the lift signals (Contd...)

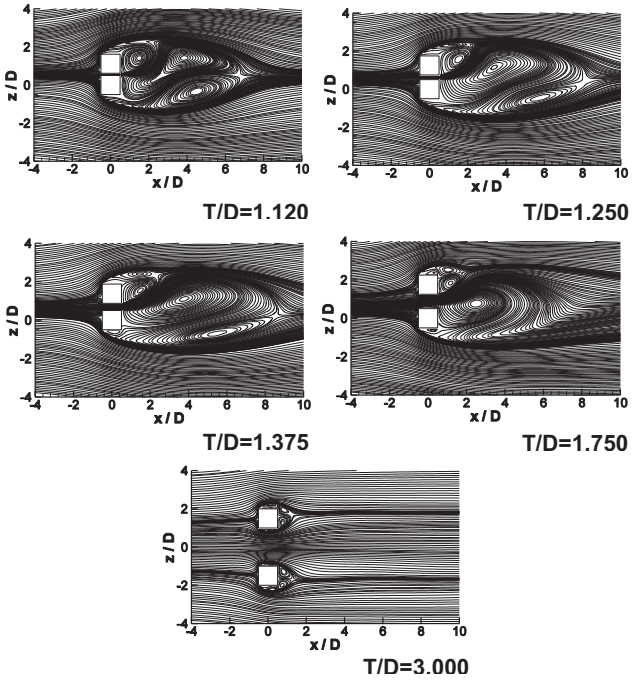

Fig. 5 Mean streamlines

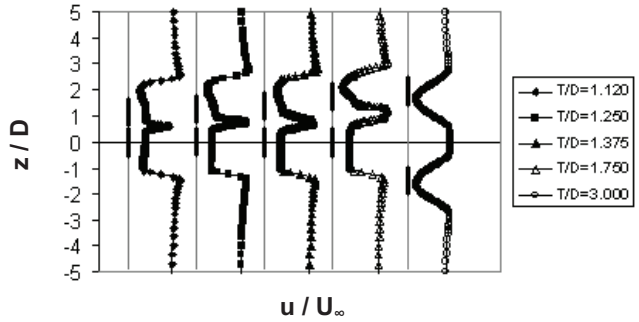

Fig. 6 Mean streamwise velocity plotted along x/D=1.0

The surface pressure distribution around the LSC and USC for all gap ratios is shown in Fig. 7. Due to the presence of the stagnation point, the pressure is maximum in the front face of both the cylinder. Except for T/D=3.0, this point is shifted away from the cylinder center for all gap ratios. This shift in stagnation point can be thought of as due to the jet-like nature of the gapside flow at smaller gap ratios. As the gap ratio increases, this shift is slowly reducing. Similar inferences can be drawn by observing the mean streamline plots (Fig. 5) as well. Another peak seen for the USC only in case of T/D=1.25 and 1.75, is due to the reattachment of the separated shear layer from the gapside leading corner to its inner surface. The mean base pressure coefficient C_{P_b} (Table 1) is defined as the pressure at the center of the rear surface of the cylinder. The USC has a lower C_{P_b} than the LSC for all gap ratios. According to Roshko, 1955 the cylinder with lower C_{P_b} value has a larger drag. This is observed to be true in the present study.

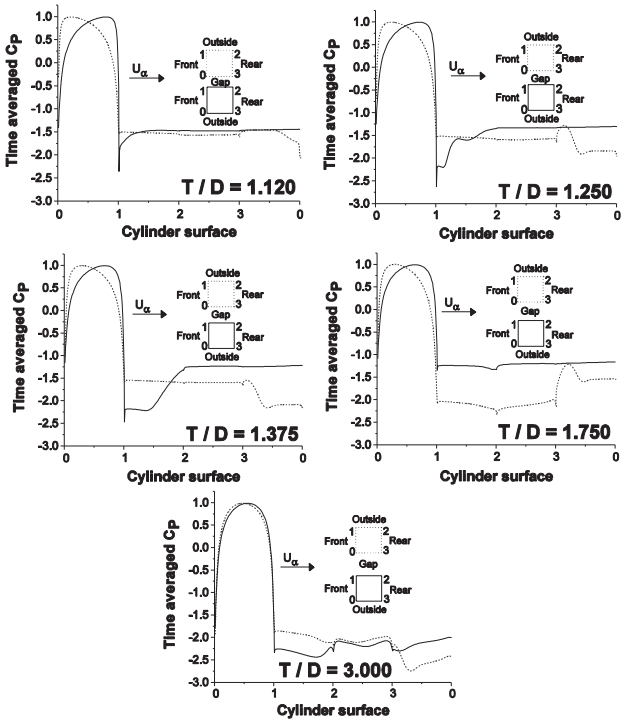

Fig. 7 Time averaged pressure coefficient

Figure 8 shows the mean streamwise velocity plotted along the respective geometric centerline for all gap ratios. On the upstream side of LSC and USC the velocity is positive and decreasing steadily as it approaches the cylinder. On the downstream side of LSC, the velocity profile first decreases and then starts to increase. This is because of the flow separation which causes a pressure drop across the

cylinder surface, leading to pressure drag and also resulting in a loss of momentum of the fluid in the wake. This is also the reason for a time averaged streamwise velocity at any point in the near wake, to be smaller than that in the free stream. After this, recovery of the velocity takes place due to entrainment of the free stream fluid. The recovery rate is directly related to the wake width. In case of USC, there is a sudden increase in the velocity profile. This is because of more momentum transferred from the biased gapside flow into the near wake of USC. After this, again a drop in the velocity profile is seen as the fluid is now moving through the wake of LSC. Then velocity recovery due to entrainment of the free stream fluid takes place.

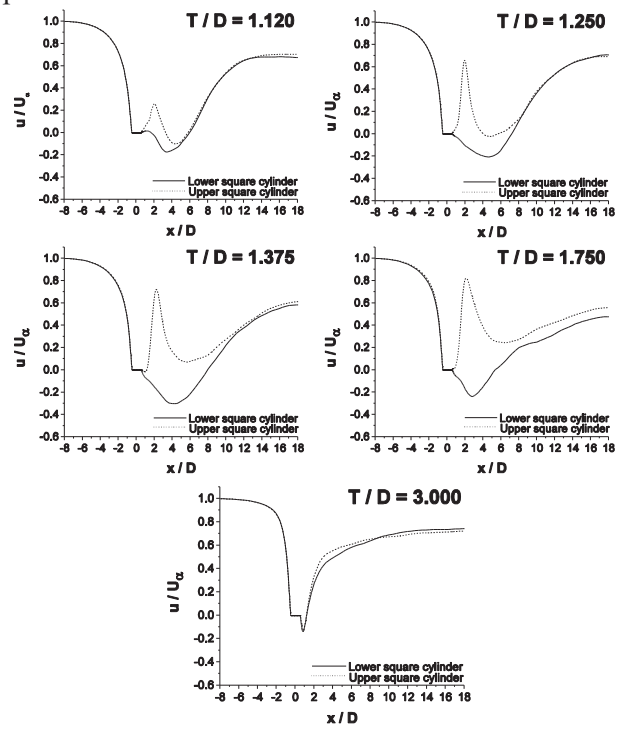

Fig. 8 Mean streamwise velocity plotted along the geometric centreline

The mean spanwise vorticity plot for all T/D ratios is shown in Fig. 9. These plots show the details of flow separation, wake formation and deflection more clearly. The merging of the separated shear layers from the bottom corner of the USC and that from the top corner of LSC, in the near wake of USC is clearly seen for T/D=1.12, 1.25, 1.375 and 1.75. Moreover, the biasing nature of the gapside flow towards the USC is also seen. At T/D=1.12 the merged shear layers from the gapside is subjected to maximum deformation because of the jet flow. The flow pattern at this gap ratio resembles that of a single bluff body flow. No merging of shear layers is found in case of T/D=3.0. This confirms the absence of interference effect for this gap ratio. According to Shao and Zhang, 2008 in case of two equal sized circular cylinders arranged side-by-side, the cylinder to which the gapside flow deflects has a higher drag coefficient. This turns out to be true for the present study, as seen in Table 1 as well as from these plots.

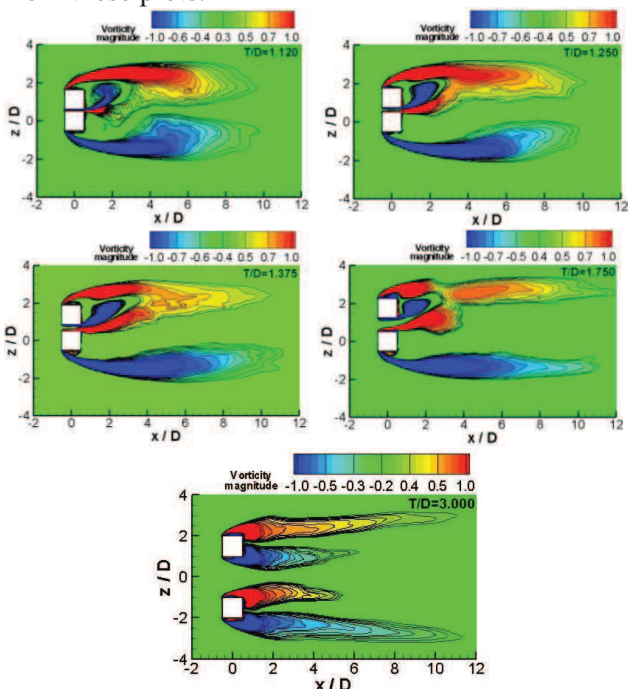

Fig. 9 Mean spanwise vorticity

CONCLUSIONS

The effect of transverse gap ratio on the flow characteristics past two ESSC in side-by-side arrangement has been carried out at Re=50000 using LES. The LSC has a higher lift coefficient for all gap ratios, except for T/D=1.75. The USC has a higher drag coefficient for all gap ratios, except for T/D=3.0. The USC has a larger value of St for T/D=1.25 and 3.0. In case of T/D=1.12, the LSC has a larger value of St. It is identical for both the cylinders in case of T/D=1.375 and 1.75. The USC has a lower mean base pressure coefficient for all gap ratios. At smaller gap ratios, the gapside flow

consists of a central jet surrounded by two shear layers separated from the top and bottom corners of the LSC and USC respectively and is more like a single bluff body flow. At T/D=3.0, the flow is very similar to that of the isolated square cylinder case. Except for T/D=3.0, the stagnation point is shifted away from the cylinder center towards the gapside for all other gap ratios. The reattachment of the separated shear layer from the gapside leading corner of the USC to its inner surface takes place for T/D=1.25 and 1.75. A biased gapside flow towards the USC is seen for all gap ratios, except for T/D=3.0.

NOMENCLATURE

C_L,C_D	Lift and Drag Coefficients
C_P	Pressure Coefficient
C_{p_b}	Mean Base Pressure Coefficient
C_s,C_k	Smagorinsky Constants
D	Diameter of the Square Cylinder
dt	Time Step
i,j,k	Index used for Tensor Notation
k_s	Turbulent Kinetic Energy
p	Pressure
Re	Reynolds Number
St	Strouhal Number
t	Non-Dimensional Time
U_∞	Free Stream Velocity
u_c	Convective Velocity
u	Streamwise Velocity
x	Streamwise Direction
y	Spanwise Direction
z	Cross-Streamwise Direction
T/D	Transverse Gap Ratio
RMS	Root Mean Square
$\bar{}$	Overbar,denote Mean Quantities
I,II	Suffix, denotes LSC and USC
< >	Filtered Quantities
ρ	Density
Δ	Filter Width (Grid Size)
υ_G	Turbulent Eddy Viscosity
τ_{ij}	Turbulent Residual Stress
δ_{ij}	Kroneckar Delta
S_{ij}	Rate of Strain Tensor of the Filtered Velocity

REFERENCES

[1] Agrawal, A., Djenidi, L., Antonia, R.A., 2006. Investigation of flow around a pair of side-by-side square cylinders using the lattice Boltzmann method, Computers and Fluids 35 1093-1107.

[2] Hirt, C.W. and Cook, J.L., 1972. Calculating three-dimensional flow around structures and over rough terrain, Journal of Computational Physics 324-340.

[3] Kolar, V., Lyn, A., Rodi, W., 1997. Ensemble-averaged measurements in the turbulent near wake of two side-by-side square cylinders, Journal of Fluid Mechanics 346 201-237.

[4] Kondo, N., 2004. Numerical simulation of aerodynamic characteristics of two rectangular cylinders in side-by-side arrangement, International Journal of Computational Fluid Dynamics 18 (5) 367 – 379.

[5] Kondo, N., Matsukuma, D., 2005. Three-dimensional computation for flow around two circular cylinders in side-by-side arrangement by a third-order upwind finite element method, International Journal of Computational Fluid Dynamics 19 (1) 37 – 43.

[6] Lankadasu, A and Vengadesan, S., 2008a. Interference effect of two equal-sized square cylinders in tandem arrangement: With planar shear flow, International Journal for Numerical Methods in Fluids 57 1005 – 1021.

[7] Lankadasu, A and Vengadesan, S., 2008b. Onset of vortex shedding in planar shear flow past a square cylinder, International Journal of Heat and Fluid Flow 29 1054 – 1059.

[8] Lankadasu, A and Vengadesan, S., 2009. Influence of inlet shear on the 3-D flow past a square cylinder at moderate Reynolds number, Journal of Fluids and Structures 25 (5) 889-896.

[9] Liu, Y. and Cui, Z.X., 2006. Three-dimensional wake interactions for two side-by-side cylinders in a cross flow, International Journal of Computational Fluid Dynamics 20 (6) 379 – 389.

[10]Nakayama, A. and Vengadesan. S.N., 2002. On the influence of numerical schemes and subgrid-stress models on large eddy simulation of turbulent flow past a square cylinder,

International Journal for Numerical Methods in Fluids 38 227-253.

[11] Niu, J. and Zhu, Z., 2006. Numerical study of three-dimensional flows around two identical square cylinders in staggered arrangements, Physics of Fluids 18 044106 (1-13).

[12] Roshko, A., 1955. On the wake and drag of bluff bodies, Journal of Aeronautical Science 22 124-132.

[13]Shao, J., Zhang, C., 2008. Large eddy simulations of the flow past two side-by-side circular cylinders, International Journal of Computational Fluid Dynamics 22 (6) 393-404.

[14]Shyam Kumar, M.B., Vengadesan, S., 2009. Large eddy simulation of flow interference between two unequal sized square cylinders, International Journal of Computational Fluid Dynamics 23 (10) 671-686.

[15]Smagorinsky, J., 1963. General circulation experiments with primitive equations, I – The basic experiment, Monthly Weather Review 91 99 – 164.

[16]Sumner, D., Wong, S.S.T., Price, S.J., Paidoussis, M.P., 1999. Fluid behaviour of side-by-side circular cylinders in steady cross-flow, Journal of Fluids and Structures 13 309-338.

[17]Sumner, D., Price, S.J., Paidoussis, M.P., 2000. Flow pattern identification for two staggered circular cylinders in cross flow, Journal of Fluid Mechanics 411 263 – 303.

[18]Wong, P.T.Y., Ko, N.W.M., Chiu, A.Y.W., 1995. Flow characteristics around two parallel adjacent square cylinders of different sizes, Journal of Wind Engineering and Industrial Aerodynamics 54/55 263-275.